Journal of Hydrology 522 (2015) 203–210

Contents lists available at ScienceDirect

Journal of Hydrology

journal homepage: www.elsevier.com/locate/jhydrol

A new approach for continuous estimation of baseflow using discrete water quality data: Method description and comparison with baseflow estimates from two existing approaches

Matthew P. Miller [a,*], Henry M. Johnson [b], David D. Susong [a], David M. Wolock [c]

[a] U.S. Geological Survey, Utah Water Science Center, 2329 Orton Circle, Salt Lake City, UT 84119, USA
[b] U.S. Geological Survey, Oregon Water Science Center, 2130 SW 5[th] Ave, Portland, OR 97201, USA
[c] U.S. Geological Survey, Kansas Water Science Center, 4821 Quail Crest Place, Lawrence, KS 66049, USA

ARTICLE INFO

Article history:
Received 6 August 2014
Received in revised form 12 December 2014
Accepted 15 December 2014
Available online 24 December 2014
This manuscript was handled by Corrado Corradini, Editor-in-Chief, with the assistance of Rao S. Govindaraju, Associate Editor

Keywords:
Baseflow
Conductivity mass balance
Specific conductance
Hydrograph separation
Groundwater

SUMMARY

Understanding how watershed characteristics and climate influence the baseflow component of stream discharge is a topic of interest to both the scientific and water management communities. Therefore, the development of baseflow estimation methods is a topic of active research. Previous studies have demonstrated that graphical hydrograph separation (GHS) and conductivity mass balance (CMB) methods can be applied to stream discharge data to estimate daily baseflow. While CMB is generally considered to be a more objective approach than GHS, its application across broad spatial scales is limited by a lack of high frequency specific conductance (SC) data. We propose a new method that uses discrete SC data, which are widely available, to estimate baseflow at a daily time step using the CMB method. The proposed approach involves the development of regression models that relate discrete SC concentrations to stream discharge and time. Regression-derived CMB baseflow estimates were more similar to baseflow estimates obtained using a CMB approach with measured high frequency SC data than were the GHS baseflow estimates at twelve snowmelt dominated streams and rivers. There was a near perfect fit between the regression-derived and measured CMB baseflow estimates at sites where the regression models were able to accurately predict daily SC concentrations. We propose that the regression-derived approach could be applied to estimate baseflow at large numbers of sites, thereby enabling future investigations of watershed and climatic characteristics that influence the baseflow component of stream discharge across large spatial scales.

Published by Elsevier B.V.

1. Introduction

Scientists and managers are often interested in identifying how watershed characteristics (e.g. geology, land use, soil type, etc.) and climatic conditions influence baseflow discharge to streams. Addressing such processes requires quantitative estimates of baseflow discharge across a gradient of watershed types. The development of quantitative methods for baseflow estimation is also necessary to understand water budgets (Stewart et al., 2007), estimate groundwater discharge (Arnold and Allen, 1999) and associated effects on stream temperature (Hill et al., 2013), and address questions of the vulnerability and response of the water cycle to natural and human-induced change in environmental conditions, such as stream vulnerability to legacy nutrients (Tesoriero et al., 2013). Given the importance of baseflow, many methods have been used to quantify the baseflow component of stream discharge beginning with Boussinesq (1877).

Approaches for baseflow estimation can be grouped into two general categories: graphical hydrograph separation (GHS) methods, which rely on stream discharge data alone, and tracer mass balance (MB) methods, which rely on chemical constituents in the stream, stream discharge, and the streamflow end-member constituent concentrations (runoff and baseflow). Many different approaches for GHS exist, including recession curve methods and digital filter methods. Recession curve methods are generally considered more objective than digital filter methods because they provide an assumed integrated signal of basin hydrologic and geologic characteristics through identification of a linear recession-constant based on the falling limb of the hydrograph (Barnes, 1939; Hall, 1968; Gardner et al., 2010). However, the ability of recession curve methods to quantify groundwater discharge to streams has been questioned because of the accuracy of the method assumptions (Halford and Mayer, 2000). Digital filter

* Corresponding author. Tel.: +1 801 908 5065.
E-mail address: mamiller@usgs.gov (M.P. Miller).

http://dx.doi.org/10.1016/j.jhydrol.2014.12.039
0022-1694/Published by Elsevier B.V.

methods either filter high frequency (assumed to be surface runoff) signals from low frequency (assumed to be baseflow) signals (Nathan and McMahon, 1990), or identify and connect successive minima on a stream hydrograph, and define baseflow as the line connecting the minima (Wahl and Wahl, 1988; Wolock, 2003). The definitions of basin-specific parameters used in these methods are generally subjective and not based on hydrologic processes (Stewart et al., 2007).

It has been suggested that MB methods for baseflow estimation are more objective than GHS because measured stream water concentrations, and either measured or estimated end-member concentrations, are related to physical and chemical processes and flow paths in the basin (Stewart et al., 2007; Zhang et al., 2013). One type of MB method that is commonly applied is the conductivity mass balance (CMB) method, which uses specific conductance (SC) as a chemical tracer for hydrograph separation. One advantage of CMB over other types of MB methods is that SC is relatively easy and inexpensive to measure. Additionally, high frequency SC measurements can be obtained using in-situ SC probes. High frequency SC data and CMB methods have been used to estimate baseflow across gradients of watershed size and land use settings (Covino and McGlynn, 2007; Miller et al., 2014; Pellerin et al., 2007; Stewart et al., 2007).

While CMB methods are generally considered to be more objective than GHS methods, their application is limited by the fact that they require high frequency SC records that are not always widely available over long time periods or spanning large numbers of watersheds. Multiple studies have developed methods to calibrate GHS estimates of baseflow to CMB estimates of baseflow (Lott and Stewart, 2013; Stewart et al., 2007; Zhang et al., 2013). Once calibrated at a specific stream location, and assuming that the end-member SC concentrations are constant over time, the GHS methods can be applied to long term stream discharge records at that location to estimate baseflow for time periods that span date ranges greater than those for which high frequency SC data are available. Li et al. (2014) showed that as little as six months of high frequency SC data can be used to calibrate a recursive digital filter model, which can then be applied to long term stream discharge records to estimate baseflow. This approach overcomes the CMB limitations associated with the lack of long-term SC records, but is only applicable at sites that have high frequency SC data available for GHS calibration. Unfortunately, high frequency SC data are not generally available at large numbers of sites within a given region. Therefore, the use of CMB, or calibration of GHS to CMB, to estimate baseflow and quantify environmental drivers of baseflow discharge across broad spatial scales is limited.

We propose that discrete SC concentration data and daily mean discharge data, which are frequently available at large numbers of sites, can be used with a CMB method to estimate baseflow at a daily time-step for the period of record of discharge data, thereby increasing the number of sites at which CMB can be used to estimate baseflow. The proposed approach involves the calibration of site-specific regression models that relate discrete SC concentrations to stream discharge and time to predict daily SC concentrations, and subsequently regression-derived CMB baseflow estimates, for the period of stream discharge record. A similar regression approach has been used to estimate water quality data, and subsequently groundwater discharge to a tropical stream for time periods when no water quality data exist (Genereux et al., 2005), but has not been applied to a number of sites and compared with other baseflow estimates from the same sites. The objective of this study is to test the proposed approach by comparing the regression-derived baseflow estimates with CMB baseflow estimates calculated using measured high frequency SC data (assumed to be the most objective estimates of baseflow) at twelve snowmelt dominated streams and rivers in the Upper Colorado River Basin (UCRB). As previously reported by Miller et al. (2014), CMB methods are well suited for estimating baseflow in snowmelt dominated watersheds. Baseflow estimates calculated using a commonly applied GHS model were also compared with measured CMB baseflow estimates.

2. Materials and methods

2.1. Site description

The UCRB is a heavily regulated watershed located in the western United States and drains an area of 294,000 km^2. The headwaters are high elevation catchments in the Rocky Mountains and the downstream end of the UCRB is located at Page, AZ, downstream of Lake Powell on the Colorado River (Fig. 1). Miller et al. (2014) estimated baseflow discharge at a daily time step for the period of record at fourteen sites draining large watersheds in the UCRB characteristic of snowmelt dominated hydrology using measured high frequency SC data with a CMB approach. As part of this process sites were screened for impacts due to anthropogenic activities. Twelve of these fourteen sites are included in the present methods comparison (Fig. 1, Table 1). Two of the fourteen sites – The Gunnison River at Delta, CO and The Uncompahgre River at Colona, CO – are not included in the present study because the short periods of record for which high frequency SC data are available at these sites resulted in a limited discrete SC data set that was not adequate for development of regression models to estimate daily SC concentrations. Drainage areas range from 1500 km^2 at PLAT to 62,000 km^2 at CO_3. Average baseflow estimates range from 1.0 ± 1.2 m^3/s to 103 ± 9.6 m^3/s, and the fraction of total streamflow estimated to be baseflow ranges from 11% to 59% (Table 1). Detailed site descriptions for these twelve locations are available in Miller et al. (2014).

2.2. Data sources

Daily mean discharge, daily mean SC, and discrete SC data were obtained from the U.S. Geological Survey (USGS) National Water Information System (NWIS) database. The date ranges for which data were acquired were limited to date ranges for which both daily mean discharge and daily mean SC data were available. Periods of records ranged from 3 to 37 years and the number of discrete samples used in regression model calibration (for estimation of daily regression-derived SC concentrations) ranged from 17 to 623 (Table 1). Detailed information regarding the periods of record, average discharge, and average SC at each site are available in Miller et al. (2014).

2.3. Regression-derived daily SC

Discrete SC values were related to daily discharge, time, and up to 7 additional variables that describe annual seasonality and variability in stream discharge of varying length. Nine different models were fitted at sites having more than 10 years of discrete SC data and 7 models were fitted at sites having less than 10 years of discrete SC data. The general form of the regression equations is described by Eq. (1). Table 2 shows the nine permutations of Eq. (1) that were used to simulate SC. Regressions were conducted in R (R Development Team, 2014).

$$\ln SC = \ln Q + \ln Q^2 + T + \sin 2\pi T + \cos 2\pi T + \sin 4\pi T + \cos 4\pi T + FA \quad (1)$$

where SC is the estimated discrete daily specific conductance (μS/cm), Q is daily discharge (m^3/s), T is time expressed as decimal years (*e.g.* 2005.25 = April 1, 2005), and FA is an additive combination of one of the groups of flow anomalies generated by

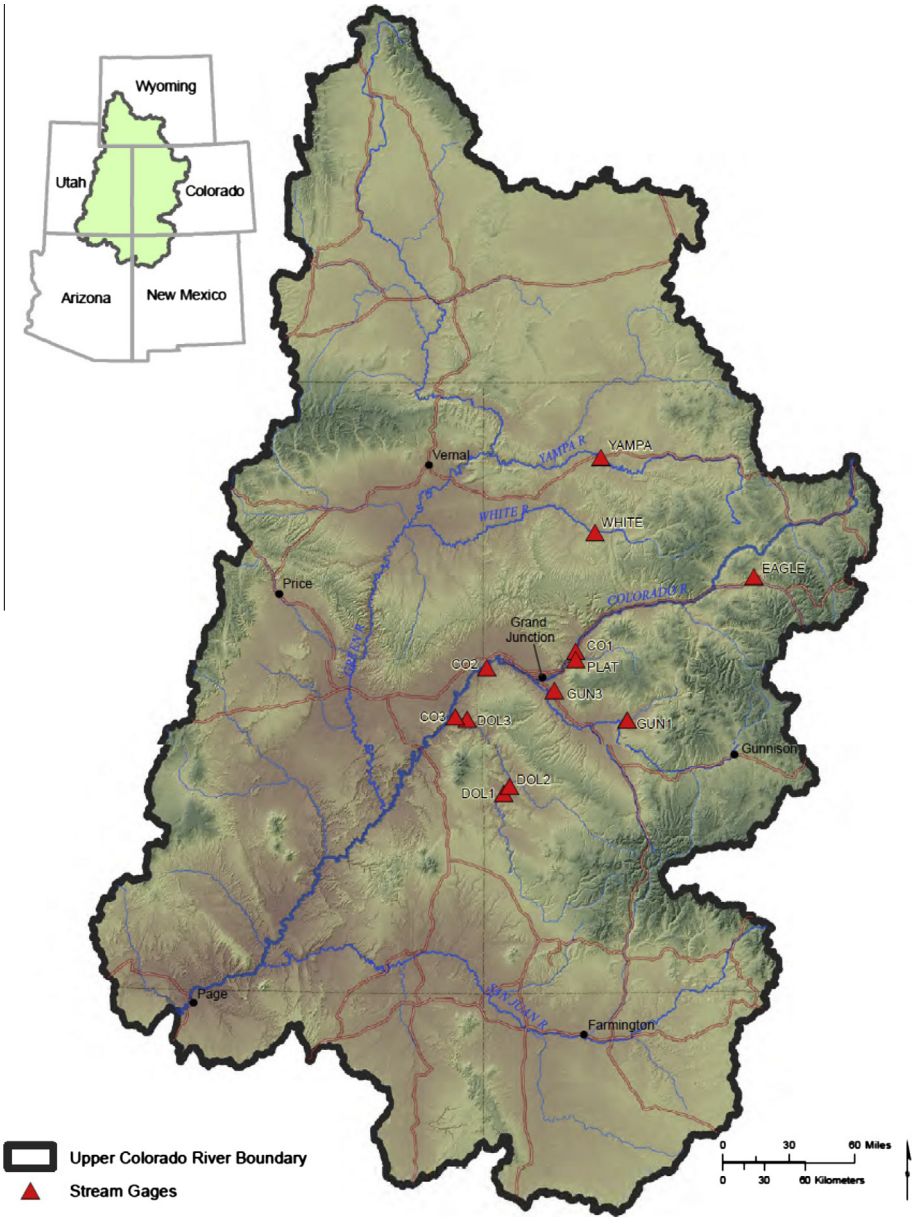

Fig. 1. Map showing the locations of the study streams in the UCRB. Inset shows the location of the UCRB in the southwestern United States.

Table 1
Period of record and number of SC values used to estimate regression-derived daily SC concentrations. Sites are listed in order of increasing drainage area.

Site ID	Site name	USGS station ID	Drainage area (km^2)	Average baseflow (m^3/s)[a]	Period of record (years)	Number of discrete SC data points used in regression model calibration
PLAT	Plateau Creek Near Cameo, CO	09105000	1533	3.0 ± 0.4 (56%)	17	165
EAGLE	Eagle River Below Milk Creek Near Wolcott, CO	394220106431500	1554	3.7 ± 0.4 (25%)	6	42
GUN1	North FK Gunnison River Above Mouth NR Lazear, CO	09136100	2510	4.5 ± 0.2 (32%)	3	17
WHITE	White River Below Meeker, CO	09304800	2652	11.9 ± 0.8 (59%)	5	245
DOL1	Dolores River at Bedrock, CO	09169500	5245	2.1 ± 0.2 (25%)	33	336
DOL2	Dolores River Near Bedrock, CO	09171100	5561	1.0 ± 1.2 (11%)	33	300
YAMPA	Yampa River Near Maybell, CO	09251000	8762	13.4 ± 2.3 (30%)	20	79
DOL3	Dolores River Near Cisco, UT	09180000	11,862	3.9 ± 0.3 (31%)	6	43
GUN3	Gunnison River Near Grand Junction, CO	09152500	20,520	39.4 ± 5.0 (57%)	37	407
CO1	Colorado River Near Cameo, CO	09095500	20,584	54.4 ± 4.5 (47%)	30	623
CO2	Colorado River Near Colorado-Utah State Line	09163500	46,229	103 ± 9.6 (55%)	33	343
CO3	Colorado River Near Cisco, UT	09180500	62,419	93.1 ± 0.4 (50%)	6	51

[a] Average baseflow from Miller et al. (2014) calculated using continuously-collected SC data. Values in parentheses are the ratio of mean baseflow to mean streamflow.

Table 2
Regression models used to generate regression-derived daily specific conductance values. '*x*' indicates that the variable was included in the model. Flow anomalies were calculated using the R package *waterData* (Ryberg and Vecchia, 2012).

Model number	Daily discharge	Daily discharge, squared	Time (T)	Seasonality		Flow anomalies									
						Group 1			Group 2			Group 3			
				Single-peak annual variability [$\sin(2\pi T) + \cos(2\pi T)$]	Dual-peak annual variability [$\sin(4\pi T) + \cos(4\pi T)$]	1 year	30 day	1 day	100 day	10 day	1 day	10 year	5 year	1 year	3 month	1 day
1	x	x	x													
2	x	x	x	x												
3	x	x	x	x	x											
4	x	x	x			x	x	x								
5	x	x	xx	x		x	x	x								
6	x	x	x						x	x	x					
7	x	x	x	x					x	x	x					
8	x	x	x									x	x	x	x	x
9	x	x	x	x								x	x	x	x	x

the R package, *waterData*, and described in the corresponding report by Ryberg and Vecchia (2012).

Annual seasonality is described using simple Fourier series that generate either one ($\sin 2\pi T + \cos 2\pi T$) or two concentration peaks per year ($\sin 2\pi T + \cos 2\pi T + \sin 4\pi T + \cos 4\pi T$). Flow anomalies (FA) are dimensionless, orthogonal time series calculated from measured daily discharge that describe the variability in stream discharge at different time scales (e.g. 1 day, 30 days, 1 year; Vecchia et al., 2008). Flow anomalies have been found to be correlated to the observed variability of concentrations of pesticides and nutrients in other studies (Vecchia et al., 2008; Ryberg et al., 2010), and therefore were expected to add significant explanatory power to the regressions used to predict SC. Table 2 shows the three different groups of flow anomalies used for this study.

The best model for each site was selected by evaluating (1) model regression diagnostic statistics, including adjusted R^2, *p*-values of the variable coefficients, and the Nash–Sutcliffe efficiency index (*E*; Nash and Sutcliffe, 1970); (2) diagnostic plots of residuals and fitted values, including fitted vs observed values, normal probability plots of model residuals, and model residuals vs the fitted values, discharge, and time; and (3) Akaike Information Criteria corrected for finite sample sizes (AIC_c) (Akaike, 1973, 1974; Hurvich and Tsai, 1989). Regression-derived daily SC values were computed using the best model identified for each site. Estimated daily SC values were corrected for retransformation bias using the correction factor of Ferguson (1986).

In addition to the model form, regression-based estimates of daily water quality are influenced by the sampling frequency and the distribution of samples with respect to season and discharge (Preston et al., 1989; Guo et al., 2002). To minimize bias and error in the regression-based estimates of SC, we verified that discrete SC samples were distributed throughout the period of record and were representative of all seasons and the range of flow conditions at each site. Discrete SC samples were collected in every year of the period of record at 10 of 12 sites; two sites, DOL1 and DOL2, had gaps of 1 year and 3 years, respectively. All sites had at least 4 samples per year for their period of record (median = 10 samples per year) and all sites had 1 or more samples per quarter for 80% of their period of record (median = 2 samples per quarter). At all sites, one or more samples were collected at discharge values exceeding the 90th percentile of the period-of-record discharge in at least 50% of the years of the period of record for the site.

2.4. Baseflow estimates

2.4.1. Graphical hydrograph separation

The widely used base-flow index (BFI) program developed by Wahl and Wahl (1988) was applied in this study to estimate baseflow from daily hydrographs, as an example GHS approach. The BFI program, which is a smoothed minima approach, is based on methods developed at the Institute of Hydrology (1980a,b). First, the daily streamflow time series is divided into *N*-day non-overlapping consecutive periods, and the minimum daily flow value within each of the *N*-day non-overlapping consecutive periods in the streamflow time series is calculated. Turning points for the baseflow hydrograph then are identified as the *N*-day minimum values that are at least 10% lower than adjacent *N*-day minimum values. These turning points are connected through linear interpolation and define the base-flow hydrograph line. Daily baseflow estimates calculated in this way are herein referred to as graphical hydrograph separation baseflow ($Q_{BF\text{-}GHS}$).

The value for *N*, which defines the width of non-overlapping periods used in the BFI method, typically is set to a value of 5 days. Wahl and Wahl (1995) point out, however, that the value of *N* can be optimized by computing the long-term average BFI value (i.e., percentage of base flow in total flow) for a range in *N* values, and then identifying the break point in the relationship between *N* and long-term average BFI values. In our study, the break point was determined for each site by (1) computing long-term average BFI values for a range (1, 2,...,30) of *N* values and then (2) using the R statistical package "segmented" (Muggeo, 2008; Muggeo and Adelfio, 2011) to determine the break point in the piecewise linear relationship. Fig. 2 shows an example break-point plot for the streamgage located at Colorado River near Cameo, Colorado (CO1).

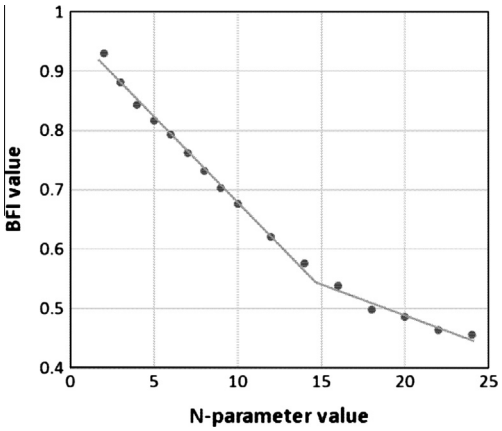

Fig. 2. Break-point analysis for the streamgage located at the Colorado River near Cameo, Colorado (CO1). The points on the graph indicate the estimated long-term average BFI values (the fraction of baseflow in total streamflow) for a range in *N*-parameter values. Using the *R* statistical package "segmented", the break-point in the piece-wise linear relationship of the points was estimated to occur at $N = 14.7$. The optimal *N*-parameter value for this site was set to 15 days (the nearest integer value).

2.4.2. Conductivity mass balance

Baseflow was estimated at a daily time step using a CMB approach (Pinder and Jones, 1969; Stewart et al., 2007):

$$Q_{BF} = Q\frac{SC - SC_{RO}}{SC_{BF} - SC_{RO}} \quad (2)$$

where Q_{BF} is base flow discharge (m^3/s), Q is total stream discharge (m^3/s), SC is the specific conductance (μS/cm) of either the measured daily mean SC or the regression-derived daily SC, SC_{RO} is the SC of the runoff end-member (μS/cm) and SC_{BF} is the SC of the baseflow end-member (μS/cm). Two different CMB baseflow estimates were generated for each day of the record at each site using Eq. (2). Daily CMB baseflow estimates calculated using the measured daily mean SC data obtained from in-situ SC probes are herein referred to as measured baseflow ($Q_{BF\text{-}MEAS}$), and daily CMB baseflow estimates calculated using the regression-derived daily SC estimates obtained from the calibration of regression models using discrete SC data are herein referred to as regression-derived baseflow ($Q_{BF\text{-}REG}$).

SC_{RO} and SC_{BF} are both estimated values. SC_{RO} represents low SC water that is delivered to the stream during snowmelt, and SC_{BF} represents the integrated SC signature from all subsurface flow paths discharging to the stream upstream of the measurement point and is high SC groundwater. Following Miller et al. (2014), SC_{RO} was defined as the average in-stream SC during snowmelt from two streams draining small high-elevation watersheds in the headwaters of the UCRB (33 μS/cm). SC_{RO} was held at a constant value of 33 μS/cm on all dates, at all sites, and for calculation of both $Q_{BF\text{-}MEAS}$ and $Q_{BF\text{-}REG}$. Unique SC_{BF} values were calculated at a daily time step for each site by calculating the 99th percentile SC concentration, which occurred during low-flow conditions, for each year of the record at each site and interpolating between these yearly values. Daily SC_{BF} values were calculated in this way using daily mean measured SC concentrations for calculation of $Q_{BF\text{-}MEAS}$, and using regression-derived daily SC concentrations for calculation of $Q_{BF\text{-}REG}$. Detailed information regarding the calculation of end-member SC concentrations, and justifications for the end-member calculation approaches are provided in Miller et al. (2014). The three assumptions regarding application of the CMB method, that is (1) contribution from other end-members are negligible, (2) end-member SC_{RO} concentrations are constant over the period of record, and (3) end-member SC concentrations are significantly different from one another (Sklash and Farvolden, 1979), are also addressed in detail in Miller et al. (2014).

2.4.3. Mean daily baseflow hydrographs

When comparing amounts and seasonal patterns in baseflow among sites and/or when investigating among-site patterns in baseflow as a function of physical watershed characteristics or climate, it is useful to have mean daily estimates of baseflow for the period of record. Mean daily baseflow hydrographs were generated by calculating mean daily $Q_{BF\text{-}MEAS}$, mean daily $Q_{BF\text{-}REG}$, and mean daily $Q_{BF\text{-}GHS}$ values for the period of record at each site (i.e. mean $Q_{BF\text{-}MEAS}$, mean $Q_{BF\text{-}REG}$, and mean $Q_{BF\text{-}GHS}$ for all $Q_{BF\text{-}MEAS}$, $Q_{BF\text{-}REG}$ or $Q_{BF\text{-}GHS}$ values estimated on January 1st, for all values estimated on January 2nd, etc. such that 365 mean values are estimated at each site for each type of baseflow estimate). Mean daily hydrographs were generated in the same way using daily measured stream discharge values.

2.5. Baseflow comparison statistics

Nash–Sutcliffe efficiency (E) values were used as measures of baseflow model fit. $Q_{BF\text{-}MEAS}$ was treated as the "observed" variable for the calculation of E, whereas $Q_{BF\text{-}REG}$ and $Q_{BF\text{-}GHS}$ were treated as the predicted variables. E values were calculated for the daily baseflow estimates for all data and separately for two seasons – snowmelt (April–July) and lowflow (August–March). The percent difference in the cumulative mean daily baseflow, from the mean daily baseflow hydrographs, was also calculated. Similar to what was done for the calculation of E values, the $Q_{BF\text{-}MEAS}$ cumulative mean daily baseflow was treated as the "observed" variable for percent difference calculations, whereas $Q_{BF\text{-}REG}$ and $Q_{BF\text{-}GHS}$ cumulative mean daily baseflows were treated as the predicted variables.

3. Results and discussion

3.1. Regression-derived daily SC

The best model selected to generate regression-derived daily SC values varied among the 12 sites; 6 different model forms were identified as the best model at one or more sites. Selected model diagnostic statistics for the best model at each site are presented in Table 3 (see Supplementary material-Appendix A for complete model diagnostic statistics for the best models). Models for all sites except EAGLE included variables for daily discharge, time, and single-peak annual variation (Table 2); EAGLE was the only site that relied on a simpler model using only daily discharge and time. At 9 of the 12 sites, additional terms capturing dual-peak annual variation or various scales of flow variability improved the regression models.

The best model was selected using the AIC_c score at 10 of the 12 sites. At sites DOL1 and DOL2, the AIC_c-selected best model had undesirable fit characteristics that were not present in one or more other models for those sites. At site DOL1, model 9 was the AIC-selected best model, however that model contained significant residual seasonal variability, predicted values were biased high compared to observed values, and only one of the four flow anomaly variables was significant at $\alpha = 0.05$. Model 3 was selected instead because it improved all of these fit characteristics and resulted in an improvement in both the adjusted R^2 and E values, while also reducing the number of variables used to fit the data. At site DOL2, model 9 was the AIC_c-selected best model, however the predicted values were biased high compared to the observed values. Model 7, a more parsimonious model, was selected instead because it improved that relation with no significant changes in other model diagnostic plots or diagnostic statistics. At all other sites, the AIC_c-selected model was deemed the best model after reviewing model diagnostic statistics and residual diagnostic plots.

Adjusted R^2 values for the best regression models ranged from 0.81 to 0.97, and E values ranged from 0.84 to 0.98 at eleven of the twelve sites (Table 3). There was a slightly poorer regression model fit at DOL1, where adjusted R^2 was 0.69 and E was 0.70.

Table 3
Diagnostic statistics for the best specific conductance regression model selected at each site. Sites are listed in order of increasing drainage area.

Site ID	AIC_c-selected model number	Best model number	Adjusted R^2	E
PLAT	3	3	0.88	0.88
EAGLE	1	1	0.97	0.98
GUN1	2	2	0.95	0.97
WHITE	3	3	0.88	0.89
DOL1	9	3	0.69	0.70
DOL2	9	7	0.87	0.87
YAMPA	9	9	0.81	0.84
DOL3	5	5	0.85	0.88
GUN3	7	7	0.91	0.91
CO1	5	5	0.95	0.95
CO2	3	3	0.96	0.96
CO3	2	2	0.94	0.94

These regression diagnostic statistics indicate that there was generally good correspondence between the measured discrete SC concentrations and the regression-derived SC concentrations. Further, diagnostic regression plots of residuals showed uniform scatter as a function of fitted values, discharge, and time (see Supplementary material-Appendix B for plots of model residuals vs fitted values and fitted vs observed values for the best models selected at each site).

3.2. Comparison of baseflow estimates

Daily $Q_{BF\text{-}REG}$ estimates were nearly identical to daily $Q_{BF\text{-}MEAS}$ estimates with the exception of three sites. Specifically, with the exception of the three Dolores River Sites (DOL1, DOL2, and DOL3), *E* values comparing $Q_{BF\text{-}REG}$ to $Q_{BF\text{-}MEAS}$ were between 0.95 and 0.99 (Table 4); indicating a near perfect fit between the $Q_{BF\text{-}REG}$ and $Q_{BF\text{-}MEAS}$ estimates. Seasonally, there was little difference between $Q_{BF\text{-}REG}$ and $Q_{BF\text{-}MEAS}$ estimates during snowmelt and during low-flow conditions at the non-Dolores River sites, with snowmelt and low-flow *E* values ranging from 0.96–0.99 and 0.85–0.98, respectively. *E* values comparing $Q_{BF\text{-}REG}$ and $Q_{BF\text{-}MEAS}$ estimates at DOL2 and DOL3 were 0.86 and 0.87, respectively; again indicating an excellent fit. There was a worse fit at DOL1, with $E = 0.45$. Taken together with the regression model diagnostic statistics (Table 3), indicating relatively poor model fit at DOL1, this result suggests that the moderately poor fit between $Q_{BF\text{-}REG}$ and $Q_{BF\text{-}MEAS}$ at this site may be due, at least in part, to the relatively poor fit obtained by the regression model.

In contrast to the excellent fit between $Q_{BF\text{-}REG}$ and $Q_{BF\text{-}MEAS}$, $Q_{BF\text{-}GHS}$ deviated from $Q_{BF\text{-}MEAS}$ at all sites. *E* values comparing $Q_{BF\text{-}GHS}$ to $Q_{BF\text{-}MEAS}$ ranged from −120 to 0.29 (Table 4), with *E* values being <0 at 9 of the 12 sites, indicating that the mean of $Q_{BF\text{-}MEAS}$ is a better predictor of baseflow than the $Q_{BF\text{-}GHS}$ estimates. $Q_{BF\text{-}GHS}$ estimates were more similar to $Q_{BF\text{-}MEAS}$ during low-flow conditions than during snowmelt at all sites with the exception of CO1 (i.e. greater *E* values during low-flow; Table 4). Fig. 3 shows an example of daily baseflow estimates obtained using the three approaches during a wet year (water year 2011) and a dry year (water year 2012) at a site where there was a good fit between $Q_{BF\text{-}REG}$ and $Q_{BF\text{-}MEAS}$ estimates (CO1) and a site with a relatively poor fit between $Q_{BF\text{-}REG}$ and $Q_{BF\text{-}MEAS}$ estimates (DOL1). At both sites the greatest deviation between $Q_{BF\text{-}MEAS}$ and $Q_{BF\text{-}REG}$ or $Q_{BF\text{-}GHS}$ occurred during the snowmelt time period.

Fig. 4 shows the mean daily baseflow hydrographs for $Q_{BF\text{-}MEAS}$, $Q_{BF\text{-}REG}$, and $Q_{BF\text{-}GHS}$, expressed as cumulative baseflow volumes. As observed for the period of record baseflow estimates, the mean daily cumulative $Q_{BF\text{-}REG}$ were more similar to the mean daily cumulative $Q_{BF\text{-}MEAS}$ than were $Q_{BF\text{-}GHS}$ at all sites. The same pattern was observed for the ratio of cumulative baseflow to cumulative streamflow (hereafter, BFI), with BFI_{MEAS} values being more similar to BFI_{REG} values than BFI_{GHS} at all sites (Table 5). The greatest deviation between mean daily $Q_{BF\text{-}MEAS}$ and mean daily $Q_{BF\text{-}REG}$ was at DOL1, where the absolute value of the percent difference between the cumulative $Q_{BF\text{-}MEAS}$ and $Q_{BF\text{-}REG}$ was 51%, followed by DOL3 and DOL2, where the percent differences were 18% and 16%, respectively (Table 5). The percent difference between the cumulative $Q_{BF\text{-}MEAS}$ and $Q_{BF\text{-}REG}$ was ⩽4% for all non-Dolores River sites. As described in Miller et al. (2014), the Dolores River runs through the Paradox Valley, where the Bureau of Reclamation has been intercepting and removing high conductivity groundwater before it discharges to the river for almost two decades (Chafin, 2003). This management action has likely resulted in short-time scale variations in baseflow discharge that

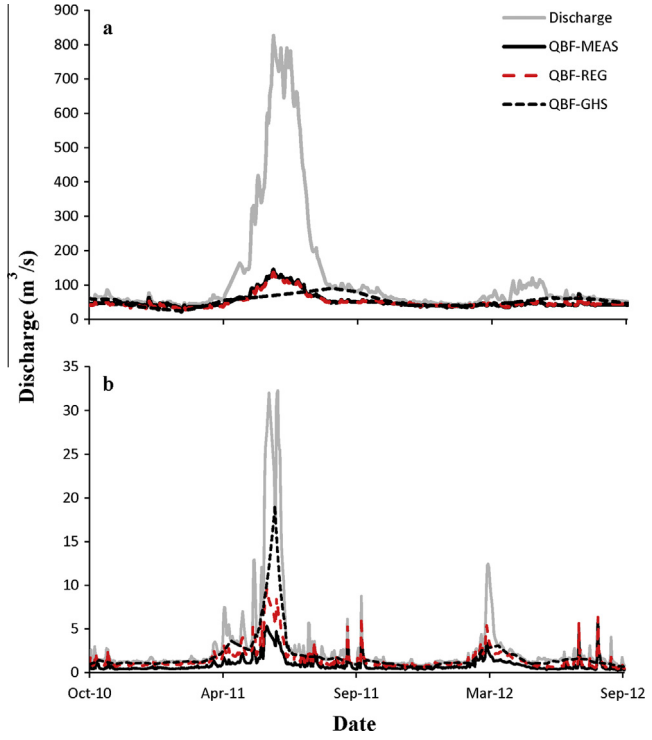

Fig. 3. Daily discharge, CMB measured baseflow (solid black line), CMB regression-derived baseflow (dashed red line), and GHS baseflow (dashed black line) for a wet year (water year 2011) and a dry year (water year 2012) at (a) CO1 and (b) DOL1. Note that the scales on the *y*-axes are variable among sites. (For interpretation of the references to color in this figure legend, the reader is referred to the web version of this article.)

Table 4
Nash–Sutcliffe Efficiency (*E*) values comparing daily CMB measured baseflow (treated as "observed" value) with daily CMB regression-derived baseflow ($Q_{BF\text{-}REG}$) and daily GHS baseflow ($Q_{BF\text{-}GHS}$) for the period of record at each site. *E* values were calculated using all data, data during the low-flow time period only, and data during the snowmelt time period only. Also shown are the *N*-parameter values used for GHS. Sites are listed in order of increasing drainage area.

Site ID	$Q_{BF\text{-}REG}$			$Q_{BF\text{-}GHS}$			*N*-parameter
	All times	Low-flow	Snowmelt	All times	Low-flow	Snowmelt	
PLAT	0.98	0.96	0.98	0.29	0.57	0.14	13
EAGLE	0.99	0.92	0.98	−0.11	−0.46	−0.93	18
GUN1	0.99	0.98	0.99	−10	0.12	−16	6
WHITE	0.99	0.94	0.99	0.07	0.39	−0.42	15
DOL1	0.45	0.47	0.34	−5.9	0.21	−9.0	6
DOL2	0.86	0.83	0.88	−120	−2.9	−200	6
YAMPA	0.99	0.97	0.98	0.20	0.49	−0.33	17
DOL3	0.87	0.81	0.85	−20	−0.05	−43	6
GUN3	0.98	0.96	0.98	−0.98	−0.18	−1.6	11
CO1	0.98	0.93	0.98	−0.19	−0.51	−0.47	15
CO2	0.98	0.95	0.98	−0.63	0.45	−1.27	13
CO3	0.95	0.85	0.96	−0.86	−0.18	−1.57	17

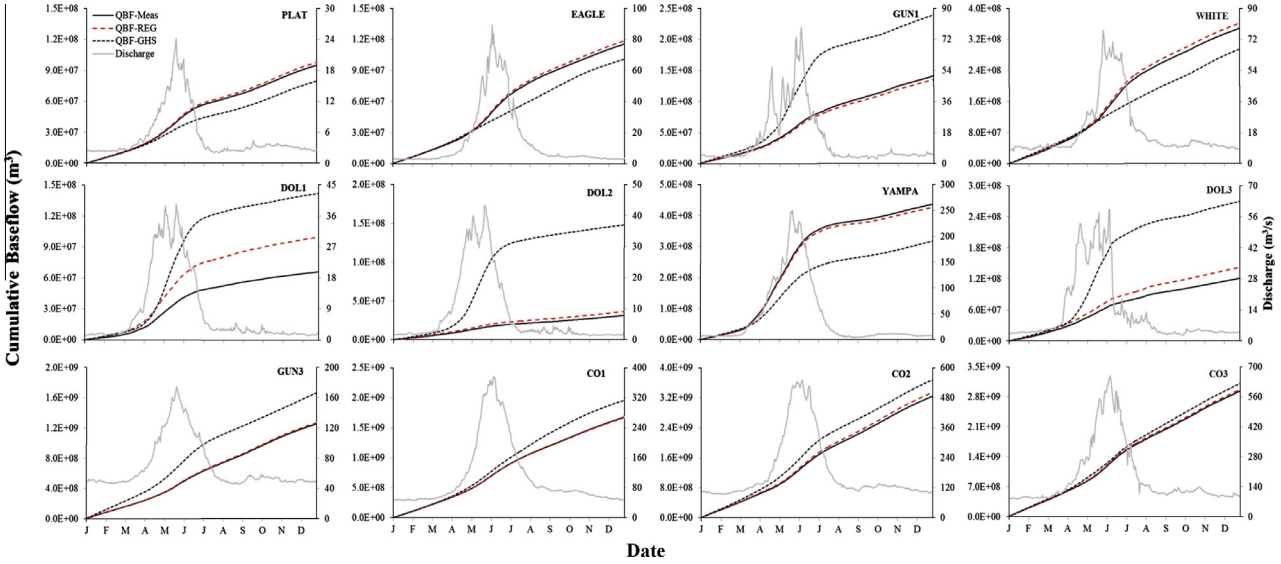

Fig. 4. Cumulative mean daily baseflow for CMB measured baseflow (solid black line), CMB regression-derived baseflow (dashed red line), and GHS baseflow (dashed black line). Mean daily stream hydrographs are also shown (solid grey line). Sites are listed in order of increasing drainage area from left to right and top to bottom. Note that the scales on the *y*-axes are variable among sites. (For interpretation of the references to color in this figure legend, the reader is referred to the web version of this article.)

Table 5
Cumulative mean daily baseflow for CMB measured baseflow ($Q_{BF\text{-}MEAS}$), CMB regression-derived baseflow ($Q_{BF\text{-}REG}$), and GHS baseflow ($Q_{BF\text{-}GHS}$). The absolute value of the percent difference between the cumulative mean daily $Q_{BF\text{-}MEAS}$ (treated as "observed" value) and $Q_{BF\text{-}REG}$ and $Q_{BF\text{-}GHS}$, as well as the BFI values obtained using the CMB measured baseflow (MEAS), CMB regression-derived (REG), and GHS hydrograph separation approaches are also shown. Sites are listed in order of increasing drainage area.

Site ID	Cumulative baseflow ($\times 10^7$ m^3)			Percent difference		BFI[a]		
	$Q_{BF\text{-}MEAS}$	$Q_{BF\text{-}REG}$	$Q_{BF\text{-}GHS}$	$Q_{BF\text{-}REG}$ (%)	$Q_{BF\text{-}GHS}$ (%)	MEAS	REG	GHS
PLAT	9.50	9.78	7.98	3.0	16	0.54	0.56	0.45
EAGLE	11.6	11.9	10.1	2.7	13	0.24	0.24	0.20
GUN1	14.1	13.6	24.0	4.0	70	0.29	0.28	0.53
WHITE	34.9	36.2	29.5	3.9	16	0.57	0.59	0.47
DOL1	6.58	9.96	14.2	51	116	0.24	0.36	0.53
DOL2	3.14	3.64	14.8	16	370	0.11	0.12	0.54
YAMPA	43.6	42.6	31.8	2.4	27	0.31	0.30	0.22
DOL3	12.1	14.2	27.0	18	120	0.28	0.32	0.65
GUN3	125	127	166	1.1	33	0.52	0.53	0.74
CO1	168	167	196	0.5	17	0.47	0.46	0.54
CO2	324	334	368	3.1	14	0.52	0.54	0.61
CO3	294	297	311	1.2	5.9	0.47	0.47	0.50

[a] BFI values calculated as the ratio of the sum of the cumulative baseflow for each hydrograph separation approach (MEAS, REG, or GHS) to the sum of the cumulative streamflow.

are difficult to account for with intermittent discrete SC samples; thereby contributing to a relatively large percent difference between the cumulative $Q_{BF\text{-}MEAS}$ and $Q_{BF\text{-}REG}$ baseflow volumes. While the Dolores River is directly impacted by the interception and removal of groundwater, all of the study sites are regulated to some degree. Taken together, these results suggest that the regression-derived baseflow estimation approach is applicable in regulated streams and rivers, but that caution is warranted when applying the approach at sites directly impacted by anthropogenic activities that alter the natural discharge and/or chemical composition of streams over short time scales.

Cumulative $Q_{BF\text{-}GHS}$ estimates deviated from the $Q_{BF\text{-}MEAS}$ estimates to a greater extent than did $Q_{BF\text{-}REG}$ at all sites. As observed for the example daily data (Fig. 3), the greatest deviation between mean daily cumulative $Q_{BF\text{-}MEAS}$ and $Q_{BF\text{-}GHS}$ occurred during snowmelt, when the slopes of the mean daily cumulative $Q_{BF\text{-}GHS}$ baseflow curves deviated most from those of the $Q_{BF\text{-}MEAS}$ curves (Fig. 4). Cumulative $Q_{BF\text{-}GHS}$ and BFI_{GHS} values were greater than $Q_{BF\text{-}MEAS}$ and BFI_{MEAS}, respectively at 8 of the 12 sites. This finding is consistent with that of Kronholm and Capel (2014), who reported that GHS estimates of baseflow were greater than CMB estimates of baseflow in a stream draining an irrigated watershed in Washington that has a single extended (~5 months) high flow season, similar to that of a snowmelt-dominated hydrograph. Cumulative $Q_{BF\text{-}GHS}$ deviated most from $Q_{BF\text{-}MEAS}$ at the Dolores River sites (116–370% difference) and at GUN1 (70% difference, Table 5), where $Q_{BF\text{-}GHS}$ and BFI_{GHS} were greater than $Q_{BF\text{-}MEAS}$ and BFI_{MEAS}, respectively. The breakpoint analysis identified *N*-parameter values of 6 as the optimal values at these four sites (Table 4). The absolute value of the percent difference between the cumulative $Q_{BF\text{-}MEAS}$ and $Q_{BF\text{-}GHS}$ values at the other sites ranged from 5.9% to 33% (Table 5), where the *N*-parameter values were between 11 and 18. These results suggest that larger *N*-parameter values (>10 days) are more appropriate than shorter values (<10 days) for estimating $Q_{BF\text{-}GHS}$ in snowmelt-dominated systems. This finding is not surprising given the extended high flow periods (e.g. 30–90 day snowmelt periods) at the study sites. Taken together these results suggest that the breakpoint analysis and subsequent estimation of $Q_{BF\text{-}GHS}$ using the Wahl and Wahl (1988, 1995) approach may not be appropriate for use in snowmelt dominated systems, and future investigations of if/how the parameters associated with this GHS approach can be calibrated to better match $Q_{BF\text{-}MEAS}$ estimates

is warranted. Comparison of CMB baseflow estimates with estimates obtained from other GHS approaches may identify GHS approaches that are more appropriate for estimating baseflow in snowmelt-dominated streams and rivers.

4. Conclusions

The results of this study demonstrate that baseflow discharge can be estimated at a daily time step for the period of record of stream discharge data using discrete SC data and daily stream discharge data. These daily baseflow estimates are obtained through the development of regression models that relate discrete SC concentrations to discharge and time, and the application of the CMB hydrograph separation method (a step-by-step summary of how the approach can be applied is provided in Supplementary material-Appendix C). There was an excellent fit between the regression-derived baseflow estimates and baseflow estimates calculated from measured high frequency SC data at those sites where the regression models were able to accurately model SC. Moreover, regression-derived baseflow estimates were more similar to baseflow estimates obtained from measured high frequency SC data than were estimates obtained using a commonly applied GHS approach. Among-site comparisons of baseflow estimates suggests that GHS *N*-parameter values of >10 days provide baseflow estimates that are more similar to high frequency SC-derived estimates than do shorter *N*-parameter values (<10 days), but that the GHS approach applied in this study may not be appropriate for snowmelt-dominated systems without further calibration of model parameters. Discrepancies between baseflow estimates obtained using measured high frequency SC data and those obtained using the regression approach at sites on a heavily managed river suggest that the regression approach should be used with caution at sites that are known to experience short time-scale variations in baseflow discharge. These results provide a new approach for estimation of baseflow that can be applied at large numbers of streams and rivers. In turn, baseflow estimates at large numbers of sites can be used to identify watershed or climatic characteristics that influence baseflow discharge to streams and rivers across large spatial scales.

Acknowledgements

We thank R. Hirsch for helpful comments on the development of the baseflow estimation approach. C. Corradini, C. Shope, and three anonymous reviewers provided valuable comments on an earlier version of this manuscript. This study was funded by the U.S. Geological Survey WaterSMART and National Water Quality Assessment Programs.

Appendix A. Supplementary material

Supplementary data associated with this article can be found, in the online version, at http://dx.doi.org/10.1016/j.jhydrol.2014.12.039.

References

Akaike, H., 1973. Information theory and an extension of the maximum likelihood principle. In: 2nd International Symposium on Information Theory. Tsahkadsor, Armenia, Akadémiai Kiadó, pp. 267–281.
Akaike, H., 1974. A new look at the statistical model identification. IEEE Trans. Autom. Control AC-19 (6), 716–723.
Arnold, J.G., Allen, P.M., 1999. Automated methods for estimating baseflow and ground water recharge from streamflow records. J. Am. Water Resour. Assoc. 35, 411–424.
Barnes, B.S., 1939. The structure of base flow recession curves. Trans. Am. Geophys. Union 20, 721–725.
Boussinesq, J., 1877. Essai sur la theorie des eaux courantes. Mem. Acad. Sci. Inst. France 23, 252–260.
Chafin, D.T., 2003. Effect of the paradox valley unit on the dissolved-solids load of the dolores river near bedrock, Colorado, 1988–2001. U.S. Geol. Surv. Water Res. Invest. Rep., 2002–4275.
Covino, T.P., McGlynn, B.L., 2007. Stream gains and losses across a mountain-to-valley transition: impacts on watershed hydrology and stream water chemistry. Water Resour. Res. 43, W10431.
Ferguson, R.I., 1986. River loads underestimated by rating curves. Water Resour. Res. 22, 74–76.
Gardner, W.P., Susong, D.D., Solomon, D.K., Heasler, H., 2010. Snowmelt hydrograph interpretation: revealing watershed scale hydrologic characteristics of the Yellowstone volcanic plateau. J. Hydrol. 383, 209–222.
Genereux, D.P., Jordan, M.T., Carbonell, D., 2005. A apired-watershed budget study to quantify interbasin groundwater flow in a lowland rain forest. Costa Rica. Water Resour. Res. 41, W04011. http://dx.doi.org/10.1029/2004WR003635.
Guo, Y., Markus, M., Demissie, M., 2002. Uncertainty of nitrate-N load computations for agricultural watersheds. Water Resour. Res. 38, 1185. http://dx.doi.org/10.1029/2001WR001149.
Halford, K.J., Mayer, G.S., 2000. Problems associated with estimating ground water discharge and recharge from stream-discharge records. Groundwater 38, 331–342.
Hall, F.R., 1968. Base flow recession, a review. Water Resour. Res. 4, 973–983.
Hill, R.A., Hawkins, C.P., Carlisle, D.M., 2013. Predicting thermal reference conditions for USA streams and rivers. Freshwater Sci. 32, 39–55.
Hurvich, C.M., Tsai, C.L., 1989. Regression and time series model selection in small samples. Biometrika 76, 297–307.
Institute of Hydrology, 1980a, Low flow studies: Wallingford, Oxon, United Kingdom, Report No. I, p. 41.
Institute of Hydrology, 1980b, Low flow studies: Wallingford, Oxon, United Kingdom, Report No. 3, pp. 12–19.
Kronholm, S., Capel, C., 2014. A comparison of continuous specific conductance-based end-member mixing analysis and a graphical method for baseflow separation of four streams in hydrologically challenging agricultural watersheds. Hydrol. Process. http://dx.doi.org/10.1002/hyp.10378.
Li, Q., Zing, Z., Danielescu, S., Li, S., Jiang, Y., Meng, F.-R., 2014. Data requirements for using combined conductivity mass balance and recursive digital filter method to estimate groundwater recharge in a small watershed New Brunswick. Canada J. Hydrol. 511, 658–664.
Lott, D.A., Stewart, M.T., 2013. A power function method for estimating base flow. Groundwater 51, 442–451.
Miller, M.P., Susong, D.D., Shope, C.L., Heilweil, V.H., Stolp, B.J., 2014. Continuous estimation of baseflow in snowmelt-dominated streams and rivers in the Upper Colorado River Basin: a chemical hydrograph separation approach. Water Resour. Res. 50, 6986–6999. http://dx.doi.org/10.1002/2013WR014939.
Muggeo, V.M.R., 2008. Segmented: an R package to fit regression models with broken-line relationships. R News 8 (1), 20–25.
Muggeo, V.M.R., Adelfio, G., 2011. Efficient change point detection in genomic sequences of continuous measurements. Bioinformatics 27, 161–166.
Nash, J.E., Sutcliffe, J.V., 1970. River flow forecasting through conceptual models. Part 1: A discussion of principles. J. Hydrol. 10, 282–290.
Nathan, R.J., McMahon, T.A., 1990. Evaluation of automated techniques for base flow and recession analysis. Water Resour. Res. 26, 1465–1473.
Pellerin, B.A., Wollheim, W.M., Fend, X., Vörösmarty, C.J., 2007. The application of electrical conductivity as a tracer for hydrograph separation in urban catchments. Hydrol. Process. 22, 1810–1818.
Pinder, G.F., Jones, J.F., 1969. Determination of the ground-water component of peak discharge from the chemistry of total runoff. Water Resour. Res. 5, 438–445.
Preston, S.D., Bierman, V.J., Silliman, S.E., 1989. An evaluation of methods for the estimation of tributary mass loads. Water Resour. Res. 25, 1379–1389.
R Development Team, 2014. The R Project for Statistical Computing (accessed 06.03.2014). http://r-project.org.
Ryberg, K.R., Vecchia, A.V., 2012. waterData – an R package for retrieval, analysis, and anomaly calculation of daily hydrologic time series data, version 1.0: U.S. Geol. Surv. Open-File Report 2012-1168.
Ryberg, K.R., Vecchia, A.V., Martin, J.D., Gilliom, R.J., 2010. Trends in pesticide concentrations in urban streams in the United States, 1992-2008: U.S. Geol. Surv. Scientific Investigations Report 2010-5139.
Sklash, M.G., Farvolden, R.N., 1979. The role of groundwater in storm runoff. J. Hydrol. 43, 45–65.
Stewart, M., Cimino, J., Ross, M., 2007. Calibration of base flow separation methods with streamflow conductivity. Groundwater 45, 17–27.
Tesoriero, A.J., Duff, J.H., Saad, D.A., Spahr, N.E., Wolock, D.M., 2013. Vulnerability of streams to legacy nitrate sources. Environ. Sci. Technol. 47, 3623–3629.
Vecchia, A.V., Martin, J.D., Gilliom, R.J., 2008. Modeling variability and trends in pesticide concentrations in streams. J. Am. Water Resour. Assoc. 44, 1308–1324.
Wahl, K.L., Wahl, T.L., 1988. Effects of regional ground water declines on streamflows in the Oklahoma Panhandle. In: Proceedings of Symposium on Water-Use Data for Water Resource Management. Tucson, Arizona, Am. Water Resour. As., pp. 239–249.
Wahl, K.L., Wahl, T.L., 1995. Determining the flow of Comal Springs at New Braunfels, Texas. Texas Water '95, American Society of Civil Engineers, August 16–17, 1995. San Antonio, Texas, pp. 77–86.
Wolock, D.M., 2003. Base-flow index grid for the conterminous United States. U.S. Geol. Surv. Open File Report 03-263.
Zhang, R., Li, Q., Chow, T.L., Li, S., Danielescu, S., 2013. Baseflow separation in a small watershed in New Brunswick, Canada, using a recursive digital filter calibrated with the conductivity mass balance method. Hydrol. Process. 27, 259–2665.